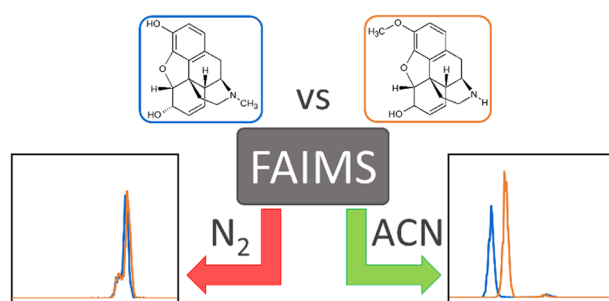**RESEARCH ARTICLE**

Effects of Solvent Vapor Modifiers for the Separation of Opioid Isomers in Micromachined FAIMS-MS

Michael S. Wei, Robin H. J. Kemperman, Richard A. Yost

Department of Chemistry, University of Florida, 214 Leigh Hall, 117200, Gainesville, FL 32611, USA

Abstract. Opioid addiction is an escalating problem that is compounded by the introduction of synthetic opiate analogues such as fentanyl. Screening methods for these compound classes are challenged by the availability of synthetically manufactured analogues, including isomers of existing substances. High-field asymmetric-waveform ion mobility spectrometry (FAIMS) utilizes an alternating asymmetric electric field to separate ions by their different mobilities at high and low fields as they travel through the separation space. When coupled to mass spectrometry (MS), FAIMS enhances the separation of analytes from other interfering compounds with little to no increase in analysis time. Addition of solvent vapor into the FAIMS carrier gas has been demonstrated to enable and improve the separation of isomers. Here we investigate the effects of several solvents for the separation of four opioids. FAIMS-MS spectra with added solvent vapors show dramatic compensation field (CF) shifts for opioid $[M+H]^+$ ions when compared to spectra acquired using dry nitrogen. Addition of vapor from aprotic solvents, such as acetonitrile and acetone, produces significantly improved resolution between the tested opioids, with baseline resolution achieved between certain opioid isomers. For protic solvents, notable CF shift differences were observed in FAIMS separations between addition of water vapor and vapors from small alcohols.

Keywords: Ion mobility, FAIMS, Solvent vapor modifiers, Opioids, Isomer separation

Introduction

Over the last three decades, the abuse of and addiction to prescription opioid analgesics has become an international health crisis. In 2016, more than 63,000 people died from drug overdoses in the USA, with about 66% of drug overdose deaths involving opioids [1]. The modern opioid crisis can generally be divided into two facets: the use of illicit opioids such as heroin and the misuse/abuse of prescription opioids [1–3]. Regarding the first, the death rate due to heroin increased 20% from 2015 to 2016. In addition, the death rate due to illicit synthetic opioids—commonly fentanyl or related compounds—increased 72% over the same time period, outpacing the death rate due to heroin for the first time since 2006 [1]. Regarding the second, it is reported that 21–29% of patients who are prescribed opioids for chronic non-malignant pain misuse them, and 40% of drug overdose deaths result from misuse/abuse of prescription opioids [1–3]. The abuse of prescription opioids can also exacerbate illicit opioid usage, as 80% of heroin addicts report starting with prescription opioids before transitioning to heroin [2, 3].

Screening for opioids typically starts with immunoassays for initial high-throughput detection and limited identification of compound class. Gas chromatography- or liquid chromatography-tandem mass spectrometry (GC- or LC-MS/MS) can be subsequently used for confirmation and more specific compound identification [4, 5]. However, the separation of opioid isomers is still challenging for GC- and LC-MS/

Correspondence to: Richard Yost; *e-mail:* ryost@chem.ufl.edu

MS methods, typically requiring extensive sample preparation and/or long chromatographic separation times. Ion mobility is an emerging technology that offers a complementary separation step and a number of advantages over traditional GC- and LC-MS/MS methods. IMS operates at the time scale in between chromatography (minutes) and mass spectrometry (μs to ms). As an additional separation step, it can reduce chromatographic separation times and increase the throughput of these methods. Finally, it can dramatically improve the separation of isomers. Recently, other groups have reported the separation of opioid isomers using high-field asymmetric waveform ion mobility spectrometry (FAIMS) coupled to mass spectrometry using minimal or no sample pretreatment [6, 7].

FAIMS, also known as differential mobility spectrometry, is a gas-phase separation technique that utilizes an asymmetric alternating electric field to filter ions by the difference between their ion mobilities at high and low fields as they traverse an analytical cell [8–10]. The ion mobility coefficient K is dependent on the size and charge of the ion. When an ion in a gas is subjected to an electric field, it will move in the direction of field lines with a velocity equal to the product of its ion mobility coefficient K and the strength of the electric field E. When the applied electric field strength is low, the mobility coefficient K is independent of the electric field strength E. However, when the applied field strength exceeds a certain threshold—about 2500 V/cm or 10 Townsends (1 Td = 10^{-17} V • cm^2) —K becomes dependent on E in a nonlinear manner that can vary between different ions [11]. The nonlinear mobility behavior at high field is generally divided into three types: type A ions gain mobility with increasing field strength, type C ions lose mobility with increasing field strength, and type B ions that initially gain mobility but eventually reverse to lose mobility with increasing field strength.

FAIMS uses a specifically designed asymmetric alternating electric field to take advantage of this nonlinear mobility behavior at different field strengths. The waveform is designed such that a high-electric field is applied for a short amount of time, followed by a lower electric field of the opposite polarity applied for a longer amount of time. The magnitude of the high-field portion is called the dispersion voltage or dispersion field (DV or DF) and is typically reported as a scale of the electric field strength. The electric field is applied orthogonal to the overall direction of ion travel. Ions will alternate moving towards one electrode or the other during each portion of the waveform. The sum of this alternating motion results in a net displacement after each waveform cycle. To be successfully transmitted, ions must essentially experience no net displacement; otherwise, they will eventually collide with an electrode and be neutralized. To transmit these ions, a DC offset termed as the compensation voltage or compensation field (CV or CF) can be applied to adjust the ion trajectory through the separation space. Different ions in a mixture can be selectively transmitted through the FAIMS cell by scanning a range of CF values. Ideally, each ion is transmitted at a unique CF value, including isomers. FAIMS has been utilized to improve the separation of different species and isomers in many compound classes, including proteins, lipids, and various small molecules [12–16].

FAIMS is still an emerging technology, and several approaches have been reported to improve its performance. One approach has been the development of different electrode geometries, which has been demonstrated to significantly affect FAIMS performance. To date, the three most commercially successful electrode geometries are those found in planar, cylindrical, and micromachined FAIMS systems, each offering their own set of advantages. Planar FAIMS geometries—which consist of two flat electrodes held parallel to each other with the analytical gap in-between—yield the highest resolution but suffer from lower sensitivity that results from losses in ion transmission through the analytical gap. Cylindrical FAIMS geometries—which consist of a cylindrical inner electrode and ring outer electrode separated by the analytical gap—have improved ion transmission and sensitivity than planar geometries that results from a focusing effect due to the non-uniform electric field in the analytical gap. However, the same non-uniform electric field results in lower resolutions when compared to planar geometries. Micromachined FAIMS geometries—which consist of an array of FAIMS channels with micrometer-sized analytical dimensions—offer the fastest analysis speeds, little added overhead time to an analysis, and a small hardware footprint. However, micromachined FAIMS geometries have much lower resolution than planar or cylindrical geometries. The low-resolution issue can be addressed by coupling micromachined FAIMS systems with another separation technique, such as chromatography, or by incorporating other FAIMS approaches for improving resolution, such as the addition of chemical modifiers into the carrier gas.

The use of chemical modifiers in the carrier gas has been previously shown to dramatically improve the resolution between FAIMS analyte peaks [16–22]. This improvement is theorized to result from ions dynamically clustering and declustering with neutral solvent molecules as the electric waveform alternates between low-field and high-field regimes [16–18, 23]. The solvent vapor effect has been demonstrated using both planar and cylindrical FAIMS geometries and across a variety of compounds classes, ranging from small molecules to large biomolecules. For example, addition of 15,000 parts per million (ppm) methanol vapor improved the resolution between ortho- and para-phthalic acid isomers to R_s = 18.3, up from 0.67 in dry nitrogen [17]. Kafle et al. improved the FAIMS separation of two deoxyguanosine adducts to DNA by adding isopropanol vapor to the carrier gas [23]. However, there is a paucity of work that combines the use of solvent vapor modifiers on micromachined FAIMS systems, and no studies have demonstrated the separation of isomeric compounds utilizing solvent vapor-modified FAIMS on such a system. The effect of solvent vapor modifiers on micromachined FAIMS analyses is not easily inferable because of the short time that ions spend in the analytical gap and the distribution of carrier gas flow through the FAIMS channel array.

In this study, we investigated the effects of several protic and aprotic solvent vapor modifiers using a micromachined FAIMS system on the separation of the [M+H]$^+$ ions of four opioids: morphine, hydromorphone, norcodeine, and codeine; three of these four compounds are isomers (morphine, hydromorphone, and norcodeine). Isomeric compounds cannot be resolved using only a single stage of mass spectrometry, thus necessitating an additional separation technique such as FAIMS. Morphine and codeine are naturally occurring opioids found in opium poppies that are widely used as analgesics and as precursor materials to many semi-synthetic opioids (e.g., hydromorphone, oxycodone, hydrocodone). In addition, several natural and synthetic opioids are metabolized to morphine by the liver, such as codeine and heroin. Hydromorphone, commonly known under its brand name Dilaudid, is an analgesic several times more potent than morphine; mistaking hydromorphone for morphine can result in overdose and death [24]. In contrast to morphine and hydromorphone, norcodeine is a metabolite of codeine and has relatively little opioid effect by itself. Norcodeine was included in this study because of its isomeric relationship, but with different chemical properties from morphine and morphine derivatives.

Experiment

Materials

Morphine, hydromorphone, norcodeine (each molecular weight 285.3), and codeine (molecular weight 299.3) standards were purchased from Cerilliant Corporation at a stock concentration of 1.0 mg/mL in methanol. Sample solutions were prepared for each individual opioid standard at a concentration of 10 µg/mL in methanol with 0.1% formic acid. Two sample solutions of 10 µg/mL morphine were prepared in either methanol with 0.1% formic acid or acetonitrile with 0.1% formic acid to investigate the effects of solution composition on FAIMS analyses. A mixture of 10 µg/mL codeine and 10 µg/mL norcodeine was also prepared for DF optimization experiments. Relatively high analyte concentrations (10 µg/mL) were used in this work for method development.

For solvent vapor addition, LC-MS grade methanol, water, acetonitrile, and ethyl acetate were purchased from Fisher Scientific, and high-purity (≥ 99%) ethanol, 1-propanol, 2-propanol, propyl acetate, and *n*-butyl acetate were purchased from Sigma-Aldrich.

FAIMS-MS Instrumentation and Methods

Experiments were conducted using a modified commercial Owlstone UltraFAIMS system interfaced to a Thermo Scientific LTQ XL linear ion trap mass spectrometer. Solutions were infused directly into the electrospray ionization source at a rate of 5.0 µL/min with no chromatographic or other separation step prior to ionization. A potential of + 5 kV was applied to the ESI emitter, and dry nitrogen sheath gas was used to assist with ionization at a flow rate of 10 arbitrary units.

The Owlstone UltraFAIMS consists of a cone interface that contains the FAIMS chip, as well as an adaptor ring that lengthens the ion source housing and connects to the FAIMS power supply. The cone interface itself is made up of the Owlstone sweep gas cone, which attaches directly to the front of the mass spectrometer, and the chip cap, which holds the FAIMS chip in place on the cone interface. The cone interface attaches directly to the LTQ spray cone and is heated by the temperature of the MS inlet capillary. For this work, the inlet capillary temperature was set to 175 °C, resulting in a FAIMS chip temperature of ~56 °C. The inlet capillary voltage was set to 10 V. An offset bias voltage of 10 V was applied to the FAIMS waveform to adjust for the inlet capillary voltage.

The inlet capillary of the chip cap was modified to improve introduction of solvent vapor. The UltraFAIMS chip cell consists of 21 parallel channels of paired gold-coated electrodes. Each channel is 4.62 mm long and has an analytical gap size of 100 µm. The separation path length is approximately 700 µm. The maximum dispersion field strength that could be applied to the FAIMS chip was 260 Td, which corresponds to a maximum dispersion voltage of about 580 V at a temperature of 56 °C and a pressure of 1 atm. FAIMS separations were performed at DFs ranging from 10 to 250 Td. The CF was scanned from − 5 to 5 Td over 60 s. FAIMS data was extracted from the mass spectra for each opioid using Thermo Xcalibur Qual Browser and processed in Microsoft Excel, R V3.3.2, RStudio V1.0.153, and MS Convert V 3.0.9134. The LTQ acquisition rate was 2.5 scans per second. Each mass spectral scan was generated from the average of 3 microscans, each with an ion injection time of 10 ms.

We define resolution for FAIMS with the equation

$$R_s = \frac{|CF_2 - CF_1|}{FWHM_{ave}} \qquad (1)$$

where R_s is the resolution; CF_1 and CF_2 are the CF peak values in Td corresponding to the analytes of interest 1 and 2, respectively; and $FWHM_{ave}$ is the average peak width in Td of analyte 1 and 2 at 50% of the full height. This is in contrast to the resolving power for FAIMS, which we define with the equation

$$R_p = \frac{|CF|}{FWHM} \qquad (2)$$

where R_p is the resolving power, CF is the CF peak value in Td, and FWHM is the average peak width in Td at 50% of the full height.

Solvent Vapor Procedure

A homebuilt apparatus for introduction of solvent vapors into the Owlstone uFAIMS cell was constructed for these experiments (Figure 1). A dry nitrogen supply was divided into two "channels," and the gas flow through each channel was regulated with a mass flow controller (MKS Instruments). Each mass flow controller was calibrated for nitrogen gas and could
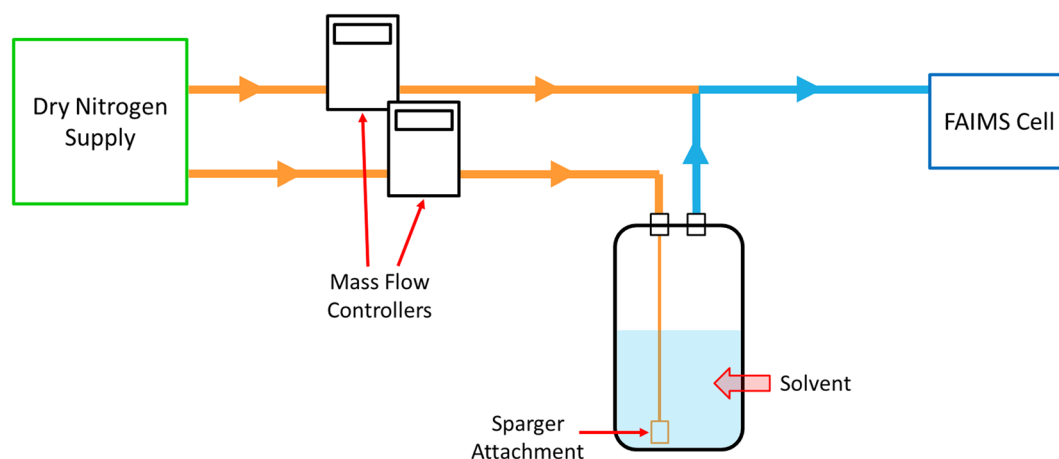
Figure 1. Schematic for solvent vapor addition apparatus. The dry nitrogen supply is split into two channels. Solvent vapor is generated by bubbling the dry nitrogen through liquid solvent using a sparger attachment in a sealed bottle. Solvated nitrogen exits the bottle through the bottle cap and then mixes with dry nitrogen from the second channel before being introduced into the FAIMS cell as the carrier gas. Gas flow through each channel is regulated using a mass flow controller

be operated from 0.5 to 5.0 L/min. Solvent vapor was generated in one channel by bubbling dry nitrogen through ~300 mL of liquid solvent using a sparger attachment in a sealed 1-L HPLC bottle at room temperature (~24 °C). Solvated nitrogen exited the bottle through the bottle cap and was then mixed with dry nitrogen from the second channel. The mixed gas was finally introduced into uFAIMS chip via the sweep gas port of the Thermo LTQ.

For our experiments, the combined gas flow from both mass flow controllers was optimized for our analytes and held constant at 2 L/min. The amount of solvent vapor introduced to the uFAIMS cell was varied by changing the ratio of solvated nitrogen flow to dry nitrogen flow while maintaining the 2 L/min combined flow. Solvent vapor concentration was calculated by measuring the loss in mass of the solvent HPLC bottle after a known amount of dry nitrogen was bubbled through the solvent. We assume that the change in mass is entirely due to evaporated solvent, and that there is no other loss of mass from the HPLC bottle. The final calculated concentrations are presented as molar fractions in parts per million (ppm) of moles of solvent molecules per total moles of nitrogen and solvent. Different vapor concentration ranges can be calculated for different solvents due to differences in vapor pressure at room temperature. More volatile solvents such as acetone produce higher vapor concentrations than less volatile solvents such as water.

Results and Discussion

FAIMS and mass spectra for morphine are presented in Figure 2. Figure 2a is obtained when dry nitrogen is used as the carrier gas, and Figure 2b is obtained when acetonitrile vapor in nitrogen is used. When using dry nitrogen, the major ion species that appear in the mass spectra for the tested opioids are the $[M+H]^+$, $[M+Na]^+$, $[2M+H]^+$, and $[2M+Na]^+$ ions, with $[M+H]^+$ as the base peak. Upon addition of solvent vapor, the

signal intensities for $[M+Na]^+$, $[2M+H]^+$, and $[2M+Na]^+$ ions decrease while the signal for the $[M+H]^+$ ion increases. In some cases, the ion corresponding to the $[M+H+solvent]^+$ can be observed, as seen in the mass spectrum in Figure 2b. For the addition of aprotic solvent vapor, the $[M+Na]^+$, $[2M+H]^+$, and $[2M+Na]^+$ ions drop below the detection limit of the mass spectrometer. Addition of acetonitrile vapor also produced narrower CF peaks widths; this phenomenon was investigated for all tested solvents and will be discussed later. Solvent vapor from sample solutions was not found to affect the FAIMS spectra for opioids in the either case where dry nitrogen is used as the carrier gas. Comparison tests between morphine sample solutions in methanol or acetonitrile show the same peaks over the same CF range with dry nitrogen carrier gas. We estimate that the vapor concentration contributed by the methanol or acetonitrile from sample solutions is less than 700 ppm.

The DF was optimized for our experiments by scanning across the values 10 to 250 Td using either a mixture of codeine and norcodeine or a mixture of morphine and norcodeine. For both sample sets, FAIMS spectra were acquired across the specified DF range with a carrier gas composition of either dry nitrogen or 8700-ppm acetonitrile vapor in nitrogen. The results of these scans for morphine and norcodeine are shown in Figure 3. When dry nitrogen is used as the carrier gas, the CF peaks for morphine, norcodeine, and codeine shift towards positive CF values as the DF strength is increased. However, their CF peaks for the $[M+H]^+$ ions are not resolved at any DF strength from 10 to 250 Td (Figure 3a, b). On the other hand, when acetonitrile in nitrogen was used as the carrier gas, the CF peaks for morphine, norcodeine, and codeine shift in the opposite direction, i.e., towards negative CF values as the DF strength is increased. This negative CF shift appears for all tested solvent vapors, corresponding to dramatic changes in the high-field mobility as a result of solvent molecule interactions with analyte ions. In addition to this difference in CF shifts, the $[M+H]^+$ ions for morphine and norcodeine begin to resolve from each other starting at a DF strength of 160 Td. At a DF of
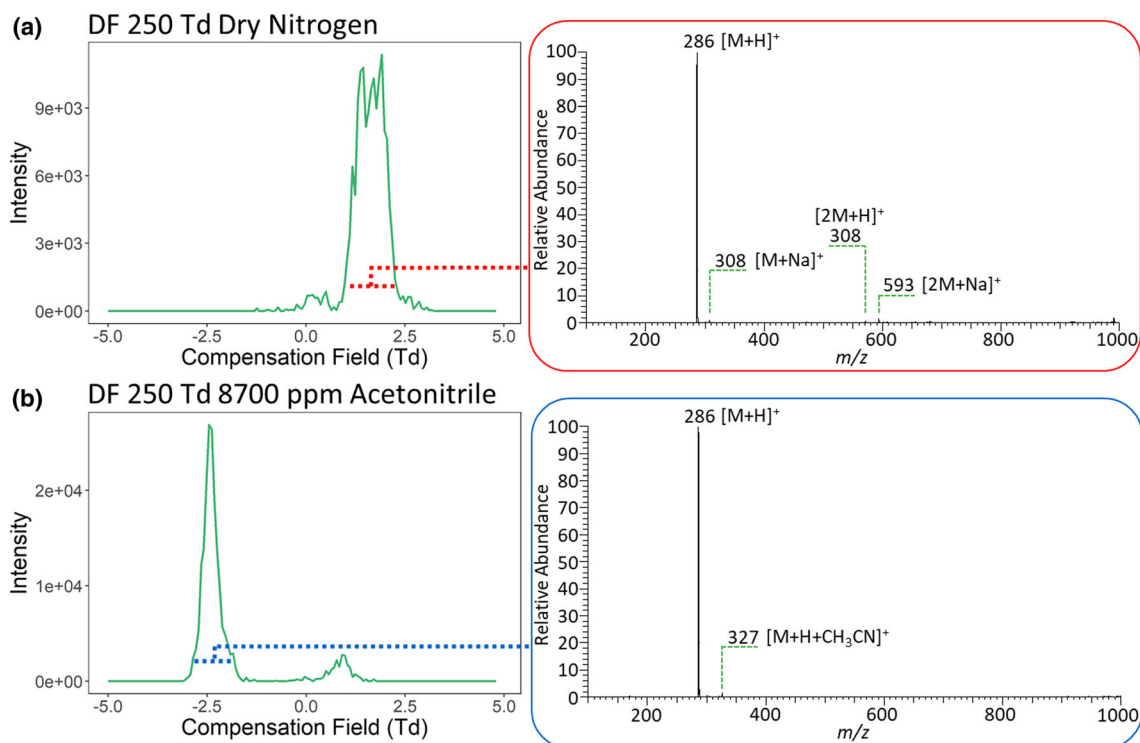
Figure 2. FAIMS spectra for [M+H]$^+$ at *m/z* 286 from a morphine solution and corresponding mass spectra acquired using either (**a**) dry nitrogen as the carrier gas or (**b**) 8700-ppm acetonitrile vapor in nitrogen as the carrier gas. The ion at *m/z* 327 corresponds to the cluster of [M+H]$^+$ with one molecule of acetonitrile ([M+H+CH$_3$CN]$^+$)

250 Td, the CF peaks for morphine and norcodeine are baseline separated with a resolution of ~2.6 (Figure 3c). Since the best separation between morphine and norcodeine was observed at a DF of 250 Td, all further data were acquired using this DF strength.

The accepted mechanism for solvent vapor effects in FAIMS is the dynamic cluster/decluster model, which stipulates that ions cluster with the vapor molecules during the low-

field portion of the FAIMS waveform and decluster to form bare ions during the high-field portion of the waveform [18, 21, 25–27]. The differences in mobility between the cluster ions at high field and bare ions at low field are significant and would require large compensation fields in order to successfully transmit the ions. Cluster ions are not observed in the mass spectra due to final declustering that occurs when the ion transitions from ambient pressure to high vacuum. The dynamic
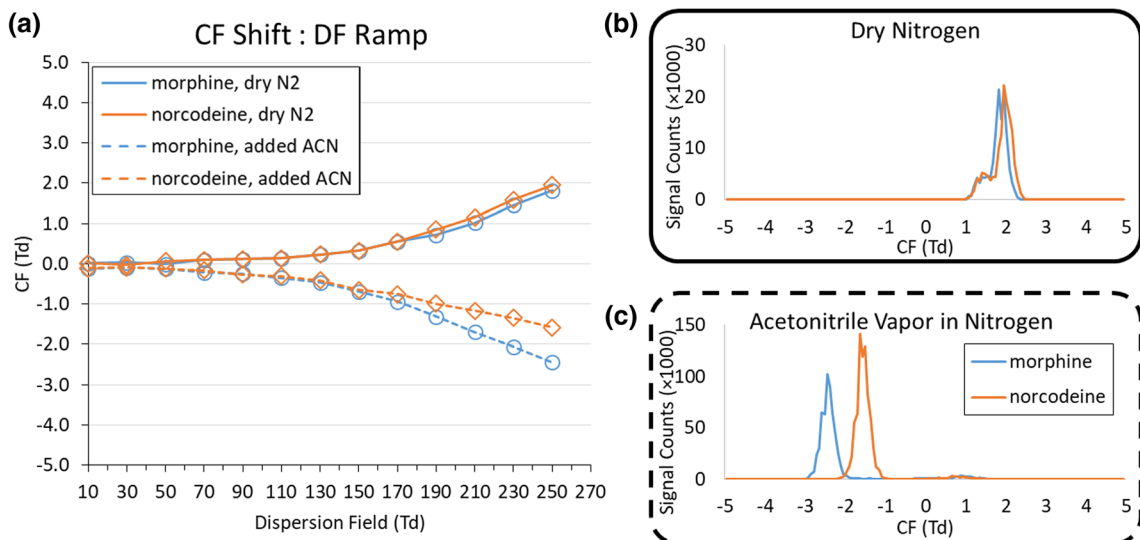

Figure 3. (**a**) Plot of CFs with increasing DFs for a mixture of morphine and norcodeine. Morphine and norcodeine begin to resolve with a DF strength of about 160 Td. The FAIMS spectra shown in (**b**) and (**c**) correspond to dry nitrogen and 8700 ppm acetonitrile at a DF of 250 Td, respectively

clustering/declustering model suggests that *m/z* values under 500 should show type A mobility behavior (where ions gain mobility with increasing field strength) when solvent vapor modifiers are used in FAIMS; the mobility of the ion species at high field—i.e., the bare ion—is higher than the mobility of the ion species at low field—i.e., the cluster ion. Ions of small molecules, such as the opioids used in this work, are believed to have type A behavior under dry nitrogen conditions. FAIMS spectra from our experiments in dry nitrogen show that the opioid CF peaks have positive CF values around 2.0 Td.

According to the dynamic clustering/declustering model, we would expect to see opioid CF peaks shift towards more positive CF values upon solvent vapor addition. However, the opposite trend is observed in our experiments. For all solvent vapors tested, we observed that the peaks shift towards negative CF values, which suggests a change in mobility behavior from type A to type C for our analyte ion species. These observations suggest that there are additional factors that cause deviation from the predictions according to the accepted model. We propose that our observations are accounted for by a solvation shell expansion/contraction mechanism that dominates over the dynamic clustering/declustering model for opioid ions. Upon introduction of solvent vapor, we assume that that a "shell" of solvent molecules forms around the ion. As the ion cluster oscillates during the FAIMS separation, the solvent shell is stable enough to survive the oscillations and "expands" during the high-field portions of the waveform, which decreases the overall mobility of the ion cluster because of a larger collisional cross section. During the low-field portions of the waveform, the ion cluster "contracts" as it returns to a rested state. The ion cluster is disrupted prior to mass analysis, most likely by turbulence due to the vacuum upon entering the mass spectrometer. As a result, the ion changes to have type C behavior (lower mobility with increasing field).

The shifts in CF peaks with increasing acetonitrile vapor concentration for the [M+H]$^+$ ions of all four opioids are shown in Figure 4a. The CF peak shifts show analogous behavior to each other with increasing acetonitrile vapor concentrations. Separation between opioids can be observed even at the lowest acetonitrile vapor concentrations (3000 ppm); only morphine and hydromorphone were not separated from each other. FAIMS spectra corresponding to 5800 ppm acetonitrile vapor concentration show near-baseline resolution between morphine and norcodeine, as well as partial resolution between morphine and codeine (Figure 4b). Mass spectrometry allows the separation of codeine from morphine because of differences in molecular weight, thus complementing the FAIMS separation. Significant overlap between the CF peaks of morphine and hydromorphone was observed for all tested concentrations of acetonitrile vapor.

The CF peaks for the [M+H]$^+$ ions of the opioids shift negatively upon introduction of any tested solvent vapor; this behavior for the [M+H]$^+$ ion of morphine is shown in Figure 5. Interestingly, we observed that the CF shifts resulting from addition of certain aprotic solvents appear to follow a trendline that is relatively independent of the specific solvent used.
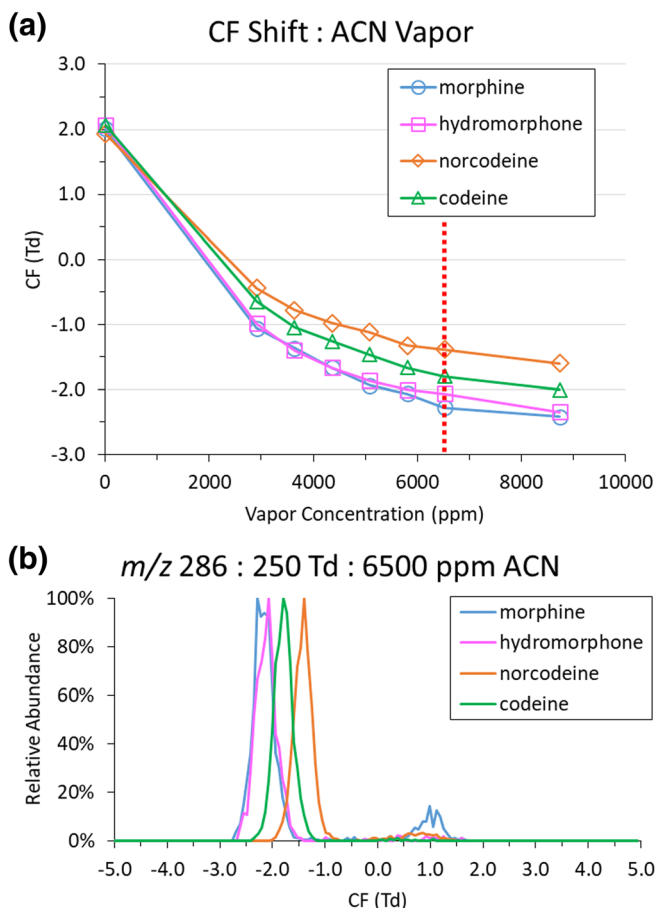

Figure 4. (**a**) Plot of CF shifts with increasing acetonitrile vapor concentration in nitrogen for the *m/z* 286 ions from four opioid solutions, along with (**b**) the FAIMS spectra for the opioid ions at an acetonitrile vapor concentration of 5800 ppm. All data were acquired at a DF of 250 Td
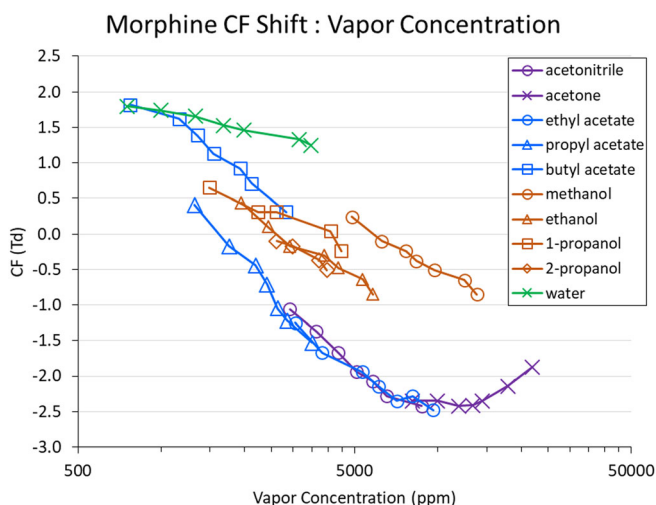

Figure 5. Plot of CF shifts with increasing vapor concentration for the *m/z* 286 ion from a morphine solution. Addition of any solvent vapor shifts the peak from positive CF values towards negative CF values. Most aprotic solvent vapors (acetonitrile, acetone, ethyl acetate, and propyl acetate) produce the same CF shifts for a given vapor concentration

As shown in Figure 5, for a DF strength of 250 Td and a vapor concentration of about 3000 ppm, the CF peak for the $[M+H]^+$ ion of morphine transmits at -1.2 ± 0.1 Td for each of the three solvents acetonitrile, ethyl acetate, and propyl acetate. When the solvent vapor concentration is about 8000 ppm, the morphine CF peak transmits at -2.4 ± 0.1 Td when using acetone, acetonitrile, and ethyl acetate. Similar results were observed for the opioids hydromorphone, norcodeine, and codeine, as will be discussed later. In contrast, addition of protic solvent vapors produced distinct CF shifts for different solvents (except 1- and 2-propanol) and do not follow the solvent-independent trendline observed with aprotic solvent vapors. These results suggest that for the addition of vapor from small aprotic solvents, the same clustering mechanism occurs for ions of an opioid, which results in the same differential mobilities for a given vapor concentration. It should be noted that the addition of *n*-butyl acetate vapor does not produce CF shifts that follow the trend exhibited by other aprotic solvents for any of the tested opioids. We hypothesize that this deviation reflects a critical threshold in one or more chemical properties (e.g., gas-phase proton affinity) that results in alternative clustering behavior to the observed trend. The molecular volume of solvent molecules, relative gas-phase basicity between opioid ions and solvent molecules, and the Gibbs free energy of different ion-solvent cluster conformations are currently being investigated.

The magnitude of the shift increases with solvent vapor concentration until about 10,000-ppm vapor in the carrier gas for acetone vapor. When the solvent vapor concentration is above this range, the rate of CF shift begins to level off and may start reversing, which can be seen for acetone vapor concentrations of 13,000 ppm and higher. This behavior is consistent with previously published results and likely extends to other solvents that follow the common clustering mechanism described previously (e.g., acetonitrile, ethyl acetate) [16, 20, 28]. We assume that a "saturated solvent shell" forms around the ion at sufficiently high vapor concentrations. At this point, the maximum CF shift is reached for that analyte and solvent. It should be noted that the maximum CF shift and reversal exhibited in the literature occurs over a very broad vapor concentration range, from 200- to 20,000-ppm solvent vapor in the carrier gas. This broad range may be accounted for by differences in the FAIMS configuration (e.g., total gas flow, FAIMS cell temperature, curved versus planar geometries).

The effects of solvent vapor on CF peak widths were also investigated and are shown in Table 1 and Figure 6. For all tested solvents, the peak widths for the $[M+H]^+$ ions of opioids narrow upon addition of solvent vapor and significantly improve the resolution of different ions in the FAIMS separation. The average full width at half maximum (FWHM) peak width for opioid CF peaks is about 0.84 Td when using dry nitrogen. The FWHM decreased to an average minimum of 0.39 Td (standard deviation $= \pm 0.06$ Td) with increasing vapor concentration for all solvents except water; adding more vapor after the minimum FWHM was reached did not appear to significantly change the peak width. It should be noted that adding water vapor produced less narrow peaks than the other solvents tested, with an average FWHM of 0.70 Td. However, the trendline for water in Figure 6 suggests that the FWHM will continue to narrow if higher concentrations of water vapor were added, possibly also reaching the same minimum peak width as the other tested solvents.

Our observations of peak narrowing with increasing vapor concentration were consistent with previous work from our lab [28]. We hypothesize that the peak narrowing results from the formation of ion clusters with a complete solvent shell resulting from deliberate addition of enough solvent vapor. As a result, the CF peak and its width are determined by only the mobility differences between the complete solvent shell of the ion at high and low fields. Increasing the vapor concentration allows the formation of larger complete shells, which produce larger CF shifts, but the formation of only complete shells keeps the variability of ion clusters low and CF peak width narrow. We also hypothesize that the opposite phenomenon occurs in cases where CF peaks broaden resulting from either very low concentrations of solvent vapor or "dry" nitrogen contaminated with uncontrolled amounts of vapor; a larger variety of ion clusters with incomplete solvent shells are formed, resulting in larger variability of ion clusters and a wider CF peak.

Across all tested solvent vapors, baseline resolution ($R_s \geq 1.5$) between morphine and norcodeine can be attained using aprotic solvent vapor concentrations as low as 1800 ppm; we achieved a resolution of 1.8 between morphine and norcodeine using vapor from propyl acetate at a concentration of 1800 ppm. Resolutions greater than 1.0 between morphine and codeine were calculated starting at a vapor concentration of ~3000 ppm acetonitrile and ethyl acetate. In contrast, the resolution between morphine and norcodeine or codeine was zero in dry nitrogen, as all analyte peaks overlapped completely with each other. Interestingly, the resolution between morphine and codeine maximizes at a vapor concentration acetonitrile and ethyl acetate around 5000 ppm, and higher vapor concentrations result in lower resolutions as the codeine CF peak shifts into and overlaps with the peak for morphine. For higher aprotic vapor concentrations represented with acetone, the resolution between morphine and codeine decreases below 0.5 at a vapor concentration of 10,000 ppm. As previously noted, partial separation of codeine from morphine is acceptable with a FAIMS-MS method, as both opioids have different molecular weights.

The resolving powers for FAIMS of opioid ions are generally higher when using aprotic solvent vapor than when using protic solvent vapor. Addition of 8700-ppm acetonitrile vapor produced resolving powers of ~7.0 for all tested opioids and were the highest resolving powers calculated in this experiment. The resolving power calculated at the largest observed CF shift occurs at ~10,000 ppm and corresponds to a resolving power of 5.0. The best resolving power for protic solvents was calculated to be 2.1 for addition of 12,000 ppm methanol. We noted that the resolving powers decrease with increasing vapor concentration for water, *n*-butyl acetate, 1-propanol, and 2-propanol. The resolving power decreases from 2.3 at dry nitrogen to 1.9 with 3500 ppm water vapor, to 0.9 with 2800 ppm *n*-

Table 1. Average FAIMS Peak Widths and Resolving Powers for Opioid [M+H]$^+$ Ions in Each Tested Carrier Gas Composition

Carrier gas	Average peak width (Td)	Standard deviation (Td)	Resolving power at highest vapor concentration	Maximum resolving power
Dry nitrogen	0.84	± 0.11	2.3 (NA)	2.3 (NA)
Water	0.70	± 0.09	1.9 (3500 ppm)	2.0 (800 ppm)
Acetonitrile	0.35	± 0.02	7.0 (8700 ppm)	7.0 (8700 ppm)
Acetone	0.50	± 0.04	4.0 (22,000 ppm)	5.3 (10,000 ppm)
Ethyl acetate	0.44	± 0.05	4.9 (9600 ppm)	5.6 (8100 ppm)
Propyl acetate	0.36	± 0.04	3.8 (3500 ppm)	3.8 (3500 ppm)
n-Butyl acetate	0.40	± 0.04	0.9 (2800 ppm)	4.1 (800 ppm)
Methanol	0.38	± 0.04	1.9 (14,000 ppm)	2.1 (12,000 ppm)
Ethanol	0.32	± 0.03	2.0 (5800 ppm)	2.0 (5800 ppm)
1-Propanol	0.40	± 0.06	0.8 (4500 ppm)	1.9 (1500 ppm)
2-Propanol	0.37	± 0.04	1.5 (4000 ppm)	1.5 (4000 ppm)

Peak widths were calculated at 50% the full height. Resolving powers are presented with associated vapor concentrations and were calculated from FAIMS spectra obtained at DF 250

butyl acetate vapor, to 0.3 with 4100 ppm 1-propanol vapor, and 0.3 with 2600 ppm 2-propanol vapor. This decrease is accounted for by the fact that the CF shifts for n-butyl acetate and water approach a CF value of 0 Td. The FAIMS performance improvement from addition of vapors from these solvents is more appropriately represented by peak widths, which narrow from 0.84 Td in dry nitrogen to 0.70 Td with water vapor, 0.40 Td with n-butyl acetate vapor, 0.40 Td with 1-propanol, and 0.37 Td with 2-propanol.

Aprotic Solvents Versus Protic Solvents

The CF shifts corresponding to opioid separation using acetonitrile, acetone, ethyl acetate, methanol, and water are shown in Figure 7; plots of the CF shifts for every tested solvent are included in the supplementary material. Opioid separation was more improved using aprotic solvents than using protic
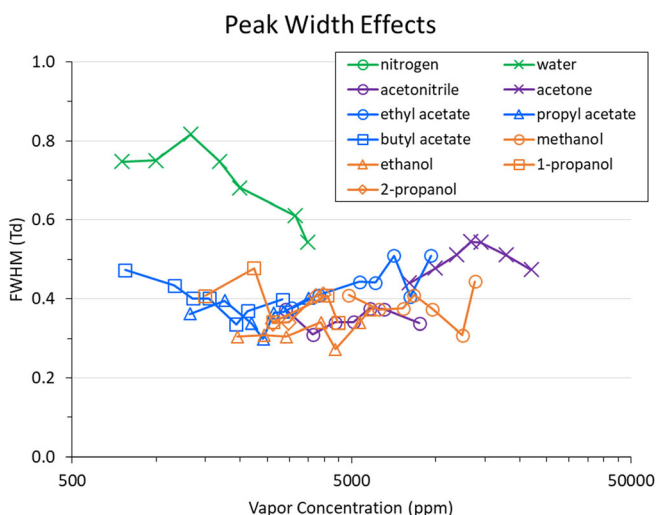

Figure 6. Plot of FAIMS peak widths with increasing vapor concentration for the m/z 286 ion from a morphine solution. The peak widths from most solvent vapors averages around 0.39 Td with a standard deviation of 0.06 Td, with water vapor being the most notable exception. Peak widths appear to broaden again when vapor concentration exceeds 7000 ppm, as can be seen with acetone vapor

solvents. For most aprotic solvents, the CF peak for morphine can be nearly baseline resolved from that of its isomer norcodeine and partially resolved from that of the analogue compound codeine. Exceptions to this trend occur with addition of propyl acetate vapor, which was unable to resolve the CF peaks of morphine and codeine, and with addition of n-butyl acetate vapor, which resulted in significant overlap between the CF peaks for morphine and norcodeine in addition to the inability to separate codeine. For protic solvents, the major CF peaks for each opioid were unresolved. CF peak intensity decreases significantly when adding vapor from water, 1-propanol, and 2-propanol.

Condensation of the solvent can be a problem for solvent vapor addition FAIMS because it causes irreproducibility in the vapor concentration and could result in hardware damage. In this work, problems due to condensation were encountered most frequently when adding vapor from water, 1-propanol, 2-propanol, and n-butyl acetate; condensate from these solvents was observed in the gas tubing even for low vapor concentrations. However, some of the CF peaks for the [M+H]$^+$ ion of opioids appear to have improved resolution at higher vapor concentrations. For example, the resolution between the [M+H]$^+$ ions of hydromorphone and morphine appears to improve at higher vapor concentrations of aprotic solvents such as acetone. One method that could enable the addition of higher vapor concentrations would be heating the solvated gas channel all the way to the FAIMS cell. The higher temperature would result in higher vapor pressure for the solvent, allowing for higher possible vapor concentrations with increased reproducibility.

A lower intensity CF peak for morphine (7–9% of base peak) can be observed in the range of 0.5 to 2.0 Td upon addition of most of the tested solvent vapors; this lower intensity peak appears to behave differently between morphine ions and hydromorphone ions. For 5800 ppm acetonitrile in nitrogen, the minor CF peak is about 11 times more intense for morphine than for hydromorphone across the same CF range (1.8×10^3 versus 0.2×10^3 signal counts, respectively). When using 9700 ppm methanol in nitrogen, the signal intensities for these minor peaks are similar (4.4×10^3 counts for morphine versus 1.5×10^3 for hydromorphone), but the transmission CF
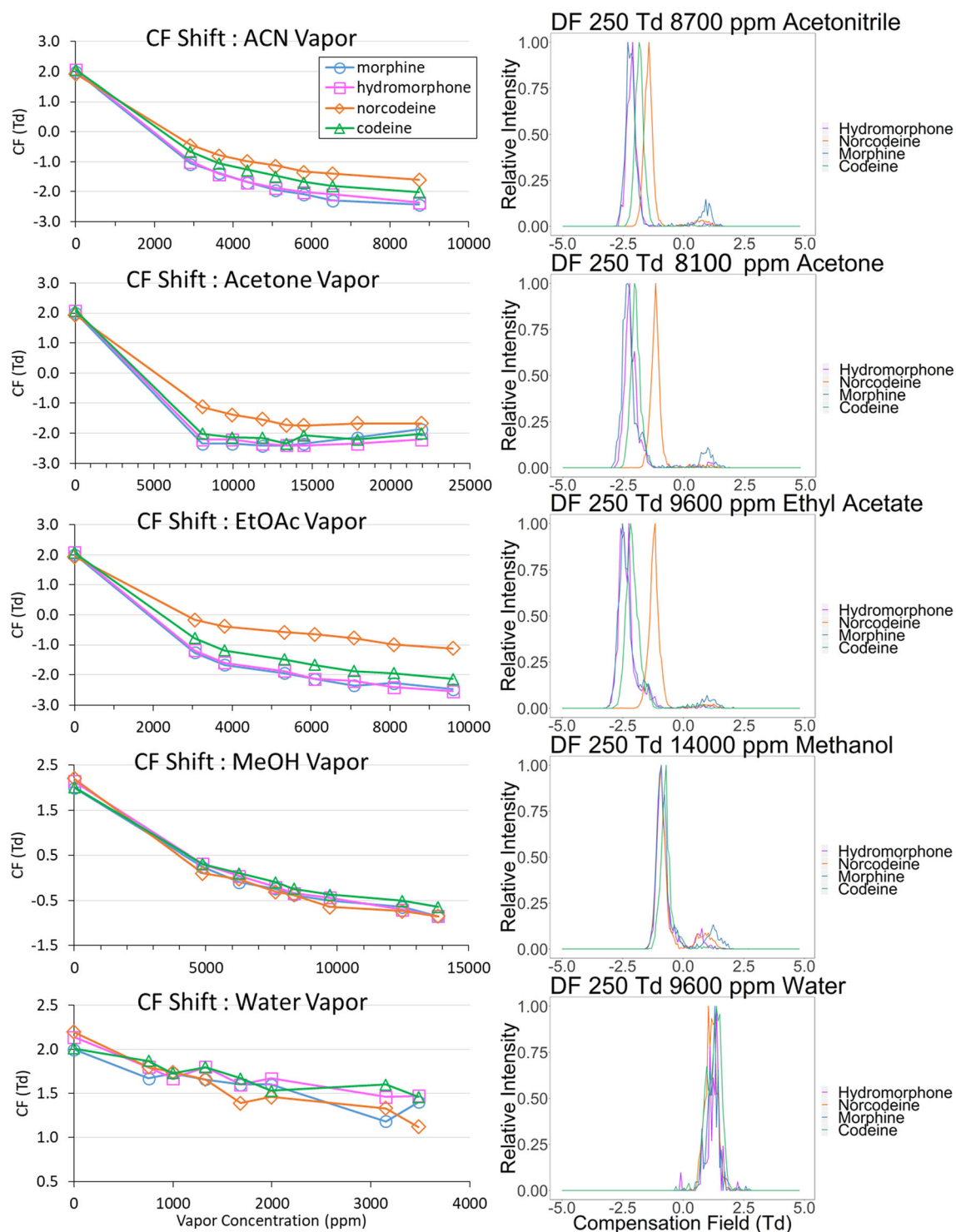
Figure 7. Plots showing CF shifts with respect to vapor concentration for acetonitrile (ACN), acetone, ethyl acetate (EtOAc), methanol (MeOH), and water (H$_2$O) for the *m/z* 286 ion from opioid standard solutions. FAIMS spectra corresponding to specific vapor concentrations are presented on the right of their respective solvent. All data were acquired at a DF of 250 Td

values are different between morphine and hydromorphone (CF 1.33 Td versus 0.85 Td, respectively). Other solvent vapors that produce notable signal for these peaks are acetone, ethyl acetate, ethanol, and 2-propanol. These minor peaks appear reproducibly with solvent vapor addition, although mass spectra taken across these peaks do not reveal a difference

in ion species from the dominant CF peak corresponding to [M+H]$^+$. Based on our previous work and reports in the literature for low-field mobility separations, we hypothesize that the minor peaks correspond to multimer ions for each opioid that fragment to monomers upon introduction to the high-vacuum environment of the mass spectrometer [9, 29, 30].
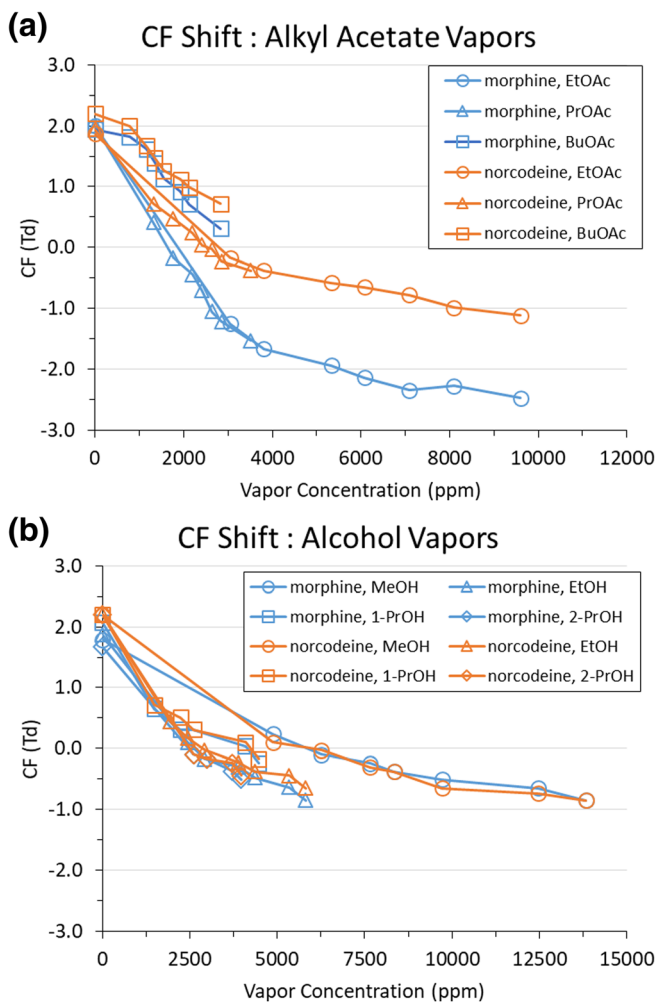
(a)

(b)

Figure 8. Plots of CF shifts with addition of vapor from (**a**) a series of alkyl acetates and (**b**) a series of alcohols for the *m/z* 286 ion from individual solutions of morphine and norcodeine. Similar CF shift behavior can be observed for both morphine and norcodeine ions. All data were acquired at a DF of 250 Td

Figure 8 shows the CF shifts corresponding to the separation of morphine and norcodeine using a series of alkyl acetates and a series of alcohols. As noted previously, the CF shifts for morphine appear to follow a trend-line and deviate from the trend for addition of *n*-butyl acetate; the same behavior is observed for hydromorphone, norcodeine, and codeine for the series of alkyl acetates. For example, addition of ethyl acetate and propyl acetate vapors also show the independent trend-line behavior for the [M+H]$^+$ ion of norcodeine as observed for the same ion of morphine. The CF shifts for the [M+H]$^+$ ion of norcodeine resolve from those for the morphine [M+H]$^+$ ion starting at a vapor concentration around 1800 ppm. In a similar manner, the CF shifts for norcodeine with *n*-butyl acetate also deviate from its smaller alkyl acetate trend and also show increasing separation from morphine at a vapor concentration around 2800 ppm. For alcohols, the CF shifts for the four tested opioids did not resolve from each other in a significant manner. Figure 8b shows the CF shifts for morphine and norcodeine from addition of alcohol vapors. While the CF shifts from

addition of ethanol and 1-propanol vapors initially appear similar to the trend-line behavior observed with addition of ethyl acetate and propyl acetate vapors, the CF shifts from addition of methanol and 2-propanol do not appear to follow any trend in common with the other alcohols.

Previous work from our lab suggested that solvents with larger molecular volumes produce CF shifts with greater magnitude [28]. Our work on the vapor addition of a series of alcohols appears to be consistent with the previous work, as the magnitude of CF shifts for opioid ions appears to increase as the size of the alcohol increases. However, we observed the opposite trend when adding vapor for a series of alkyl acetates; as the size of the alkyl acetates increases, the magnitude of CF shifts decreases. This opposite pattern suggests that there are factors in addition to molecular volume that affect the magnitude of CF shifts when adding solvent vapor to FAIMS. It is likely that the clustering mechanism that causes the solvent-independent trend-line observed with aprotic solvent vapors also results in the opposite pattern observed for a series of alkyl acetates. Because the intermolecular interactions between molecules of aprotic solvents are weaker than those of protic solvents, the shell made from larger aprotic solvent molecules may be broken more easily during the FAIMS separation. This would produce a smaller "expanded" ion cluster during the high-field portion and lower magnitude CF shifts relative to the case where a smaller aprotic solvent were added. In contrast, protic solvent molecules are able to create stronger interactions via gas-phase hydrogen bonding and allow the shell to remain intact. Larger protic molecules produce a bigger expanded ion cluster during the high-field portion and larger-magnitude CF shifts as a result.

Conclusions

Integrating rapid ion mobility separations into current mass spectrometry screening methods would increase confidence in compound identification and sample throughput, and even micromachined FAIMS systems are capable of significantly improving the selectivity of isomers when combined with supporting approaches, such as addition of solvent vapor modifiers. Selection of the solvent vapor that produces optimal separation is heavily dependent on the target analytes. As a result, solvent vapor-modified FAIMS is best employed for targeted analyses. We have investigated and reported how various aprotic and protic solvents can affect the FAIMS separation of several opioid compounds, including the isomers morphine, hydromorphone, and norcodeine. These opioid isomers could not be separated from each other using dry nitrogen carrier gas in FAIMS. Addition of vapor from small aprotic solvents produced the best separation between opioids, which also appeared to produce CF shifts that follow a trend-line independent of the specific identity of the solvent. Identification of the chemical or physical properties that account for the trend-line behavior may improve our fundamental

understanding of high-field ion mobility and are currently being investigated.

Addition of solvent vapor also produces several other analytical benefits in addition to enhanced selectivity, including increased analyte transmission through the FAIMS cell, higher signal intensities, and narrower peak widths, each as observed previously in our lab. Increasing vapor concentration initially broadens CF peak widths, followed by peak narrowing after a sufficient concentration of solvent vapor has been reached. At high enough vapor concentrations, peak widths appear to approach a minimum width that is hypothesized to result from mobility differences as the solvent shell of the ion cluster expands and contracts during the FAIMS separation. Peak widths reach a minimum when enough solvent vapor is present to form a complete solvent shell. Larger CF shifts can be obtained with increasing vapor concentration even after peak widths reach a minimum. Increasing the vapor concentration allows the formation of larger complete shells, which produce larger CF shifts, but the formation of only complete shells keeps the variability of ion clusters low and CF peak width narrow.

The performance of FAIMS depends on the geometry and instrumentation of the system. Increasing the residence time of analyte ions in the FAIMS cell can lead to improved resolving power and could reduce the amount of solvent vapor required to produce separation. Developing a robust and reliable solvent vapor addition system is critical for reproducible vapor-modified FAIMS separations. Adequate temperature control of the solvent vapor reduces the risk of condensation in the system, which causes inaccuracy in vapor concentration measurements and analyte signal intensities. Future research efforts aim at elucidating the changes in solvent vapor-modified FAIMS separations for structurally similar molecules.

Acknowledgements

References

1. Hedegaard, H., Warner, M., Minino, A.M.: Drug overdose deaths in the United States, 1999–2016. NCHS Data Brief. **294**, 1–8 (2017)

2. Kolodny, A., Courtwright, D.T., Hwang, C.S., Kreiner, P., Eadie, J.L., Clark, T.W., Alexander, G.C.: The prescription opioid and heroin crisis: a public health approach to an epidemic of addiction. Annu Rev Public Health. **36**, 559–574 (2015)

3. Vowles, K.E., McEntee, M.L., Julnes, P.S., Frohe, T., Ney, J.P., van der Goes, D.N.: Rates of opioid misuse, abuse, and addiction in chronic pain. Pain. **156**, 569–576 (2015)

4. Gergov, M., Nokua, P., Vuori, E., Ojanperä, I.: Simultaneous screening and quantification of 25 opioid drugs in post-mortem blood and urine by liquid chromatography-tandem mass spectrometry. Forensic Sci Int. **186**, 36–43 (2009)

5. Pergolizzi, J., Pappagallo, M., Stauffer, J., Gharibo, C., Fortner, N., De Jesus, M.N., Brennan, M.J., Richmond, C., Hussey, D.: The role of urine drug testing for patients on opioid therapy. Pain Pract. **10**, 497–507 (2010)

6. Manicke, N.E., Belford, M.: Separation of opiate isomers using electrospray ionization and paper spray coupled to high-field asymmetric waveform ion mobility spectrometry. J Am Soc Mass Spectrom. **26**, 701–705 (2015)

7. Liu, C., Gómez-Ríos, G.A., Schneider, B.B., Le Blanc, J.C.Y., Reyes-Garcés, N., Arnold, D.W., Covey, T.R., Pawliszyn, J.: Fast quantitation of opioid isomers in human plasma by differential mobility spectrometry/mass spectrometry via SPME/open-port probe sampling interface. Anal Chim Acta. **991**, 89–94 (2017)

8. Buryakov, I.A., Krylov, E.V., Nazarov, E.G., Rasulev, U.K.: A new method of separation of multi-atomic ions by mobility at atmospheric pressure using a high-frequency amplitude-asymmetric strong electric field. Int J Mass Spectrom Ion Process. **128**, 143–148 (1993)

9. Purves, R.W., Guevremont, R., Day, S., Pipich, C.W., Matyjaszczyk, M.S.: Mass spectrometric characterization of a high-field asymmetric waveform ion mobility spectrometer. Rev Sci Instrum. **69**, 4094–4105 (1998)

10. Schneider, B.B., Nazarov, E.G., Londry, F., Vouros, P., Covey, T.R.: Differential mobility spectrometry/mass spectrometry history, theory, design optimization, simulations, and applications. Mass Spectrom Rev. **35**, 687–737 (2016)

11. Yousef, A., Shrestha, S., Viehland, L.A., Lee, E.P.F., Gray, B.R., Ayles, V.L., Wright, T.G., Breckenridge, W.H.: Interaction potentials and transport properties of coinage metal cations in rare gases. J Chem Phys. **127**, 154309–154319 (2007)

12. Shvartsburg, A.A., Danielson, W.F., Smith, R.D.: High-resolution differential ion mobility separations using helium-rich gases. Anal Chem. **82**, 2456–2462 (2010)

13. Bowman, A.P., Abzalimov, R.R., Shvartsburg, A.A.: Broad separation of isomeric lipids by high-resolution differential ion mobility spectrometry with tandem mass spectrometry. J Am Soc Mass Spectrom. **28**, 1552–1561 (2017)

14. Shvartsburg, A.A., Bryskiewicz, T., Purves, R.W., Tang, K., Guevremont, R., Smith, R.D.: Field asymmetric waveform ion mobility spectrometry studies of proteins: dipole alignment in ion mobility spectrometry? J Phys Chem B. **110**, 21966–21980 (2006)

15. Šala, M., Lísa, M., Campbell, J.L., Holčapek, M.: Determination of triacylglycerol regioisomers using differential mobility spectrometry. Rapid Commun Mass Spectrom. **30**, 256–264 (2016)

16. Purves, R.W., Ozog, A.R., Ambrose, S.J., Prasad, S., Belford, M., Dunyach, J.-J.: Using gas modifiers to significantly improve sensitivity and selectivity in a cylindrical FAIMS device. J Am Soc Mass Spectrom. **25**, 1274–1284 (2014)

17. Rorrer, L.C., Yost, R.A.: Solvent vapor effects on planar high-field asymmetric waveform ion mobility spectrometry. Int J Mass Spectrom. **300**, 173–181 (2011)

18. Schneider, B.B., Nazarov, E.G., Covey, T.R.: Peak capacity in differential mobility spectrometry: effects of transport gas and gas modifiers. Int J Ion Mobil Spectrom. **15**, 141–150 (2012)

19. Schneider, B.B., Covey, T.R., Nazarov, E.G.: DMS-MS separations with different transport gas modifiers. Int J Ion Mobil Spectrom. **16**, 207–216 (2013)

20. Beach, D.G.: Differential mobility spectrometry for improved selectivity in hydrophilic interaction liquid chromatography-tandem mass spectrometry analysis of paralytic shellfish toxins. J Am Soc Mass Spectrom. **28**, 1518–1530 (2017)

21. Schneider, B.B., Covey, T.R., Coy, S.L., Krylov, E.V., Nazarov, E.G.: Chemical effects in the separation process of a differential mobility/mass spectrometer system. Anal Chem. **82**, 1867–1880 (2010)

22. Hall, A.B., Coy, S.L., Nazarov, E.G., Vouros, P.: Rapid separation and characterization of cocaine and cocaine cutting agents by differential mobility spectrometry-mass spectrometry. J Forensic Sci. **57**, 750–756 (2012)

23. Kafle, A., Coy, S.L., Wong, B.M., Fornace, A.J., Glick, J.J., Vouros, P.: Understanding gas phase modifier interactions in rapid analysis by differential mobility-tandem mass spectrometry. J Am Soc Mass Spectrom. **25**, 1098–1113 (2014)

24. Grissinger, M.: Morphine and hydromorphone: an omnipresent risk of mix-Ups. P&T. **33**, 194–247 (2008)

25. Krylova, N., Krylov, E.V., Eiceman, G.A., Stone, J.A.: Effect of moisture on the field dependence of mobility for gas-phase ions of

organophosphorus compounds at atmospheric pressure with field asymmetric ion mobility spectrometry. J Phys Chem A. **107**, 3648–3654 (2003)

26. Eiceman, G.A., Krylov, E.V., Krylova, N.S., Nazarov, E.G., Miller, R.A.: Separation of ions from explosives in differential mobility spectrometry by vapor-modified drift gas. Anal Chem. **76**, 4937–4944 (2004)

27. Levin, D.S., Vouros, P., Miller, R.A., Nazarov, E.G., Morris, J.C.: Characterization of gas-phase molecular interactions on differential mobility ion behavior utilizing an electrospray ionization-differential mobility-mass spectrometer system. Anal Chem. **78**, 96–106 (2006)

28. Rorrer, L.C., Yost, R.A.: Solvent vapor effects in planar high-field asymmetric waveform ion mobility spectrometry: solvent trends and temperature effects. Int J Mass Spectrom. **378**, 336–346 (2015)

29. Chouinard, C.D., Cruzeiro, V.W.D., Roitberg, A.E., Yost, R.A.: Experimental and theoretical investigation of sodiated multimers of steroid epimers with ion mobility-mass spectrometry. J Am Soc Mass Spectrom. **28**, 323–331 (2017)

30. Campbell, J.L., Yang, A.M.C., Melo, L.R., Hopkins, W.S.: Studying gas-phase interconversion of tautomers using differential mobility spectrometry. J Am Soc Mass Spectrom. **27**, 1277–1284 (2016)